Journal of The Electrochemical Society, **159** (2) J29-J33 (2012)
0013-4651/2012/159(2)/J29/5/$28.00 © The Electrochemical Society

Low-Temperature Synthesis of $Sr_2Si_5N_8$:Eu^{2+} Red-Emitting Phosphor by Modified Solid-State Metathesis Approach and Its Photoluminescent Characteristics

Artavazd Gh. Kirakosyan and Duk Young Jeon[z]

Department of Materials Science and Engineering, Korea Advanced Institute of Science and Technology, Daejeon 305-701, Korea

$Sr_2Si_5N_8$:Eu^{2+} red-emitting nitridosilicate phosphor was prepared by a low temperature modified solid-state metathesis (MSSM) approach. The method is based on the nitridation of strontium chloride in presence of silicon and lithium nitrides. Lithium nitride was used as a solid source of nitrogen and as reduction agent for strontium chloride. We revealed that the formation of $Sr_2Si_5N_8$ occurs via solid+liquid mechanism through intermediate $SrSiN_2$ phase and found that $Sr_2Si_5N_8$:Eu^{2+} can be synthesized by MSSM approach starting at a considerably low temperature (1100°C). We first showed the possibilities of using flux materials during the synthesis of complex alkaline earth-based nitridosilicates. The phosphor particles synthesized at optimized condition (1300°C and 6 hours) show a rod-like morphology in 1–5 μm width and 5–10 μm length. The color coordinate (CIE) of $Sr_2Si_5N_8$:Eu^{2+} (2 wt%) are (0.6382; 0.3612) and emission spectrum exhibits a broad-band peaking at 628 nm. The synthesized phosphor was applied to LED package and white light has been obtained with CCT ∼ 4700 K and R_a ∼ 90–92 depending on driving current. The MSSM method has proven to be a cost-effective and facile way to prepare nitridosilicate phosphor with outstanding performance. An approximate chemical pathway for $Sr_2Si_5N_8$:Eu^{2+} formation is proposed.
 [DOI: 10.1149/2.058202jes]

Manuscript submitted September 16, 2011; revised manuscript received November 7, 2011. Published December 19, 2011.

In recent years, nitridosilicate-based down-conversion phosphors have been widely used in LED lighting[1,2] and have attracted much attention due to their valuable properties, such as their exceptional thermal and chemical stability.[3,4] Intense luminescence was observed in rare-earth element doped silicon nitride-based materials, e.g. α-SiAlON:Eu^{2+}, Ce^{3+},[5,6] β-SiAlON:Eu^{2+},[7] $MSi_2O_{2-\delta}N_{2+2/3\delta}$:$Eu^{2+}$,$Ce^{3+}$ (M = Ca, Sr and Ba),[8,9] $M_2Si_5N_8$:Eu^{2+},Ce^{3+} (M = Ca, Sr and Ba),[10–23] $CaAlSiN_3$:Eu^{2+},[24,25] and $SrAlSiN_3$:Eu^{2+}.[26] Owing to wide broadband excitation under near-UV to blue light, silicon nitride-based phosphors are excellent candidates for multiple applications in combination with near-UV/Blue LED chips. Among known nitridosilicate phosphors, $Sr_2Si_5N_8$:Eu^{2+} offers high quantum efficiency and low thermal quenching, making it the most promising red-emitting component for adjusting the color rendering index for white light-emitting diodes (w-LEDs).

Considerable effort has been directed toward the development of an efficient synthesis route for the $Sr_2Si_5N_8$:Eu^{2+} phosphor. Notable suggestions for nitride synthesis have included conventional solid-state reactions (SSR),[10,11] carbothermal reduction and nitridization (CRN),[13,15–19] and a high temperature calcination method.[14] However, the aforementioned methods have various disadvantages, in that the required initial reactants are extremely sensitive to oxygen and moisture. On the other hand, the most of preparation methods require high pressure and temperature more than 1500°C in the reaction zone and a prolonged heating period. Therefore the development of a low temperature, pressureless, facile, and efficient route for the synthesis of a high-performing $Sr_2Si_5N_8$:Eu^{2+} red-emitting phosphor is urgent.

Low temperature synthesis of $Sr_2Si_5N_8$ nitridosilicate has been explored and reported by several researchers. Schnick and co-workers reported a single source based low temperature (>900°C) synthesis method for a $Sr_2Si_5N_8$:Eu^{2+} nitridosilicate where the precursor is processed by dissolving metal into ammonia under high pressure ∼300 bars.[22] However, further heat-treatment at a high temperature to improve its photoluminescence emission was also required. Schnick and co-workers also successfully created a reaction between a microcrystalline metal amide precursor ($Sr(NH_2)_2$) and silicon di-imide ($Si(NH)_2$) at 1300–1400°C to produce $Sr_2Si_5N_8$.[23] These developments have demonstrated the possibility of synthesizing the nitridosilicate phases, in particularly $Sr_2Si_5N_8$ at relatively low temperatures, as compared with common synthesis conditions (1450–1650°C).[22,23]

[z] E-mail: dyj@kaist.ac.kr

Among the metal nitride synthesizing methods we addressed to the low-temperature metathesis reactions, which seems to be more promising not only for the binary nitride phase synthesis,[27] but also for synthesizing complex nitrides, including nitrosilicate ones.

In this study, we have studied the synthesis peculiarities of $Sr_2Si_5N_8$:Eu^{2+} phosphor by modified solid-state metathesis approach. Therefore, a new reaction system of Li_3N-$SrCl_2$-Si_3N_4-Eu_2O_3 composition was designed and investigated upon the time and the heat treatment temperature.

Experimental

All raw materials (anhydrous $SrCl_2$, α-Si_3N_4, Li_3N, and Eu_2O_3) with 99.9% purity were purchased from Sigma-Aldrich. The mixing procedure was performed in a glove box filled with Ar gas. About 2.0–3.0 g of as-prepared powder mixture was loosely filled in an alumina crucible and non-isothermally heat-treated in a tubular furnace under nitrogen/hydrogen (80/20 mol%) gas flow. The samples were heated with a heating rate of 5°/min to the predetermined temperature (900–1400°C) and kept at maximum temperature for 0–20 hours. Then, t*he* crucible with the sample was allowed to cool naturally to room temperature and then was removed from the pipe furnace. The reaction product was preliminary grinded into a fine powder and subjected to an acid leaching in order to eliminate the reaction by-products. After leaching the sediment was rinsed with warm distilled water and dried in a vacuum oven at 80°C for 2 h.

Phase composition analysis were carried out using an X-ray diffractometer (Rigaku D/max IIIC, Rigaku, Japan) with Cu Kα (λ = 1.542 A°) and an electron dispersive X-ray analyzer (NOVA 230). The morphology of powders was evaluated using a scanning electron microscope (S-5000, Hitachi Ltd., Tokyo, Japan). The photoluminescence spectra was recorded at room temperature using a fluorescence spectrophotometer (F-7000, Hitachi Ltd., Tokyo, Japan) with a 150 W Xe lamp as an excitation source. The quantum efficiency was determined by integrated sphere method. Thermal quenching was tested by using PTE-VUVD2L-100 equipment. TGA was performed with a Setaram 92-18.

Results

TG analysis for particular binary systems such as $SrCl_2$-Si_3N_4, Li_3N-Si_3N_4, and $SrCl_2$-Li_3N were conducted in N_2 atmosphere in order to determine the contribution of individual reactions in the overall

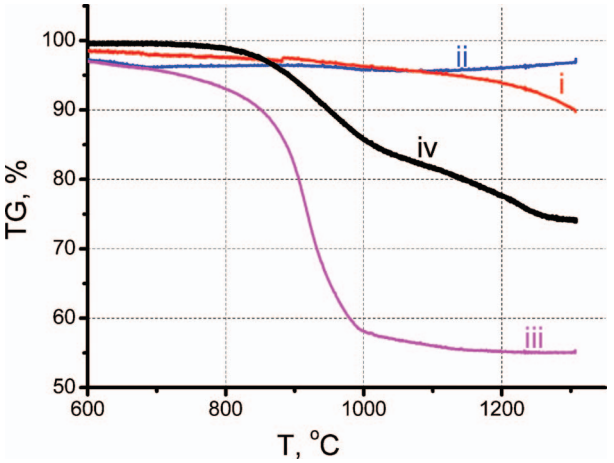

Figure 1. TG analysis of starting powder mixture for four different particular cases, i) $SrCl_2$-Si_3N_4, ii) Li_3N-Si_3N_4, iii) $SrCl_2$-Li_3N, iv) $SrCl_2$-Si_3N_4-Li_3N.

synthesis process. The analysis results are shown in Fig. 1. Minor weight loss in $SrCl_2$-Si_3N_4 system (curve i) until 1200°C is recorded. However, above this point weight lost rate become essentially accelerated. Meantime no weight change is recorded in Li_3N-Si_3N_4 binary system (curve ii) at the entire temperature range. In contrast to the previous cases, $SrCl_2$-Li_3N system (curve iii) shows abrupt weight loss (45%) starting with 820°C. Weight loss more likely was originated by chemical reaction between $SrCl_2$ and Li_3N resulting Sr_3N_2 and volatile LiCl. TG analysis of as-designed $SrCl_2$-Li_3N-Si_3N_4 (curve iv) complex mixture also shows essential weight loss started around 820°C identical to $SrCl_2$-Li_3N binary system. At that about 27–30% weight loss was recorded by TG analysis. Based on TG analysis data we can conclude that intensive chemical reactions in $SrCl_2$-Li_3N-Si_3N_4 system were started above 800°C.

Fig. 2 shows SEM micrographs and EDS analysis of the samples prepared at 1300°C for 0.5, 1, and 1.25 hours. After 0.5 h heat treatment, small size crystals (point 1) and partially melted agglomerates (point 2) could be detected. EDS analysis at marked points shows Si and N (point 1), and Sr, O, and Cl (point 2). Shown in point 1 small crystals continuously grow up (point 3) and finally transform to the micrometer sized rod-like crystals (point 4). The main elements detected at the point 3 and 4 are Sr, Si and N. However, traces of O and Cl can be also detected after 1.25 h of processing.

Fig. 3 shows XRD patterns of the reaction products prepared at 1300°C for 0, 1, 1.25, 2 hours. When keeping time in the maximum point is 0 h, XRD patterns indicate the existence of $LiSi_2N_3$, $SrCl_2$, and Sr_4OCl_6 (JCPDS-70-3183, 75-1623, 86-1832, respectively) (Fig. 3a). Here, the formation of Sr_4OCl_6 may be related to the oxygen in Eu_2O_3 phase. Increasing the duration of the processing to 0.5–1 h (b), resulted a small change in phase composition: along with the main constituents a small portions of LiCl (JCPDS-74-1972) and $SrSiN_2$ (JCPDS-22-1438) were also formed. Notable change in phase composition was observed after 1.25 h processing (Fig. 3c): the characteristic peaks of the $Sr_2Si_5N_8$ (JCPDS 85-0101) were appeared on XRD patterns. Prolonging of the firing process resulted sharp peaks of $Sr_2Si_5N_8$ phase, indicating its well-crystalline nature (Fig. 3d). Note that, the formation period of $Sr_2Si_5N_8$ phase become prolonged at lower calcination temperatures. For instance, according to our experiments, the formation period of $Sr_2Si_5N_8$ phase at 1100°C was prolonged to 12 h.

Based on the results of EDS and XRD analysis we can suppose that the small crystals observed at point 1 of Fig. 2 is $LiSi_2N_3$ (Li cannot be detected by EDS). The partially molten mass in point 2 (Fig. 2), may be identified as a $SrCl_2$ and Sr_4OCl_6. The crystals at the point 3 may be identified as $LiSi_2N_3$ coexisting with $SrSiN_2$. The rod-like crystalline grains at the point 4 mainly are $Sr_2Si_5N_8$ nitridosilicate.

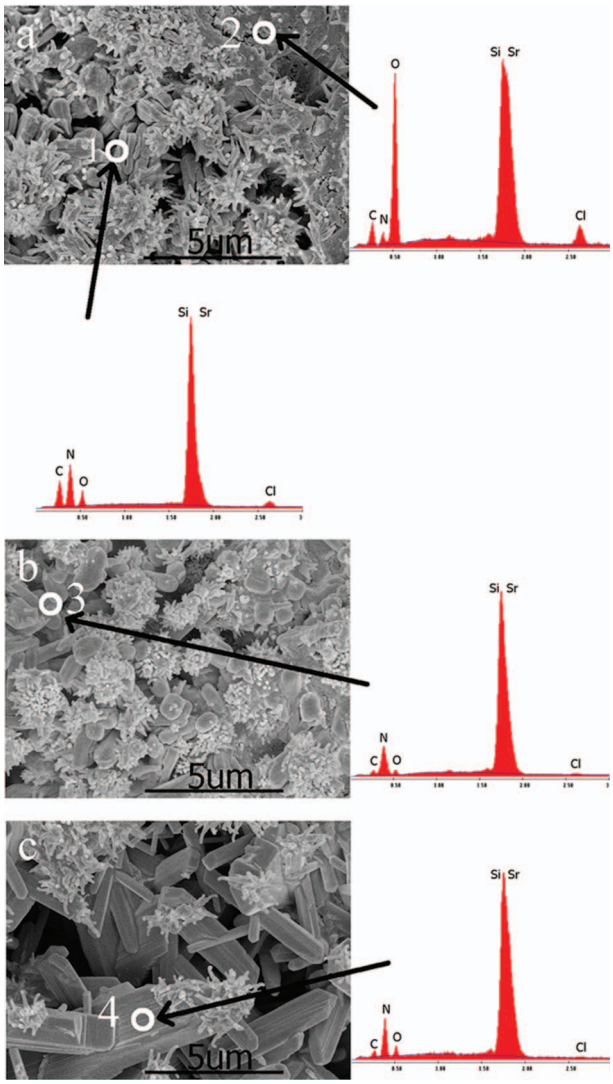

Figure 2. SEM images and EDS analysis of the samples fired at 1300°C for different durations, (a) 0.5, (b) 1, and (c) 1.25 h.

Fig. 4 shows the XRD pattern of phosphor powder synthesized at 1300°C for 6h. As can be seen, most of the aforementioned intermediate phases ($SrCl_2$, Sr_4OCl_6, LiCl and $SrSiN_2$) were completely disappeared from the XRD patterns (Fig. 4a). A small portion of $LiSi_2N_3$ remained in the final product was eliminated by subsequent acid washing (Fig. 4b). Moreover, it was shown that the existence of $LiSi_2N_3$ at 1300°C (at 6 h) was related with partially evaporation of $SrCl_2$ from the reaction zone. Therefore, after adding an extra portion of $SrCl_2$ (10–15%) to the reaction, we obtained product containing $Sr_2Si_5N_8$ and trace amount of LiCl. Purification of the product by warm distilled water resulted single phase $Sr_2Si_5N_8$, as shown in Fig. 4c.

Fig. 5 shows the SEM micrographs of $Sr_2Si_5N_8$ powder prepared at 1300°C for 6 h without and with excess of $SrCl_2$. As can be seen in both cases product particles have well developed crystalline (rod-like) shape. However, excess of $SrCl_2$ yields nitridosilicate grains with bigger size and smooth surface. These crystals are approximately 1–5 μm in diameter and more than 5 μm in length. After the grinding and acid rinsing the particles became optically improved, well dispersed and the average size of grains was reduced to 5–10 μm.

Fig. 6 illustrates the PL emission spectra of samples versus the processing time. As can be seen, the sample heat treated at 1300°C for 0.5 and 1.0 h shows two emission spectra peaking around 450 and

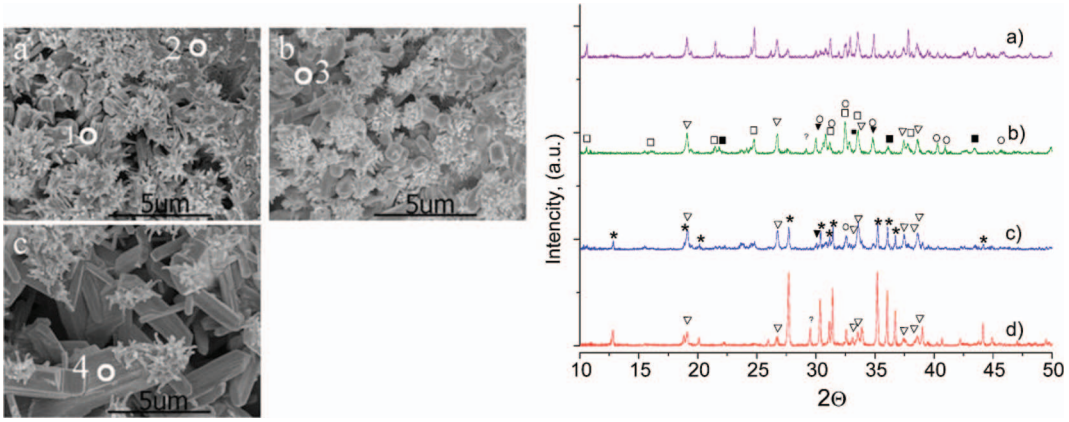

Figure 3. X-ray diffraction patterns of samples fired at 1300°C for different durations, (a) 0 h, (b) 1 h, (c) 1.25 h, (d) 2 h, ■-$SrCl_2$, □-Sr_4OCl_6, ○-$SrSiN_2$, ▼-LiCl, ∇-$LiSi_2N_3$, *-$Sr_2Si_5N_8$, ?–unidentified peak.

700 nm under $\lambda_{ex} = 290$ nm excitation (curves a and b). These two emission peaks are related with $Sr_4OCl_6:Eu^{2+}$[28] and $SrSiN_2:Eu^{2+}$[29] phosphor phases, respectively. Extending the process duration to 1.25 h (curve c) brings to abrupt transition of $SrSiN_2:Eu^{2+}$ to $Sr_2Si_5N_8:Eu^{2+}$ red-emitting phosphor, therefore new emission peak at 628 nm characterizing $Sr_2Si_5N_8:Eu^{2+}$,[10–23] can be seen on the emission spectra. Meantime, the peak at 700 nm completely disappeared from the spectra. Further increasing the processing time enhances the emission intensity at 628 nm. Meantime the emission peak at 450 nm decrease continuously and after 2 hours treatment only single peak at 628 nm can be detected (curve e).

Fig. 7 shows the effect of temperature on the emission intensity of $Sr_2Si_5N_8:Eu^{2+}$ phosphors. Here, Figs. 7a and 7b shows PL intensity of phosphor samples before and after purification, respectively. Simple comparison shows that purified from LiCl samples show 10–15% higher intensity compared to unpurified one.

The PL intensity of the phosphor obtained at optimized condition is about 115–116% of that of a reference YAG:Ce^{3+} yellow phosphor (Mitsubishi, 00902). At room temperature, the full-width at half-maximum (FWHM) is observed to be about 95 nm, which is wider by 3–10 nm than of those reported previously for $Sr_2Si_5N_8:Eu^{2+}$.[11,12,22,23] External and internal quantum efficiencies of synthesized powder are 62 and 75% respectively, these values agree to that reported previously.[11,14] Thermal stability assignment showed that PL intensity at 175°C maintain about 89–90% of initial value of that measured at room temperature, which is slightly higher than that provided in literature.[11,16,21] The Commission Internationale de L'Eclairage (CIE) chromaticity coordinates (x, y) are (0.6382; 0.3612). The synthesized phosphor was applied to LED package for warm-white light application purposes. Phosphor prepared by MSSM method was combined with blue LED chip ($\lambda_{em.} = 450$ nm) and Eu^{2+} doped $SrSi_2O_{2-\delta}N_{2+2/3\delta}$ and $BaSi_2O_{2-\delta}N_{2+2/3\delta}$.[8,9] White light has been obtained with correlated color temperature (CCT) around 4700 K and Ra ~90–92 depending on driving current. The PL spectrum of the sample synthesized at 1000°C cover the emission $SrSiN_2:Eu^{2+}$ phosphor,[29] but the origins of the widening to deep red diapason is not clear yet. Our finding will be published later.

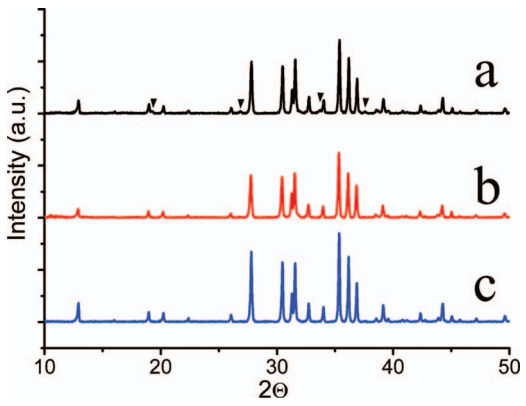

Figure 4. X-ray diffraction patterns of samples, (a) fired at 1300°C for 6 h, (b) fired at 1300°C for 6 h (after acid-washing), and (c) fired at 1300°C for 6 h with excessive of $SrCl_2$ ▼-$LiSi_2N_3$.

Discussion

Based on the obtained data, the overall chemical reaction between anhydrous strontium chloride ($SrCl_2$), lithium nitride (Li_3N), and silicon nitride (Si_3N4) may be schematically presented as follows:

$$SrCl_2 + Li_3N + Si_3N_4 \rightarrow Sr_2Si_5N_8 + LiCl \quad [1]$$

The reaction process can be divided in several stages.

Stage 1: Melting of Li_3N and interaction with Si_3N_4 to form $LiSi_2N_3$:[31] (800–900°C)

$$Li_3N(liq) + Si_3N_4(sol) \rightarrow LiSi_2N_3(sol) \quad [2]$$

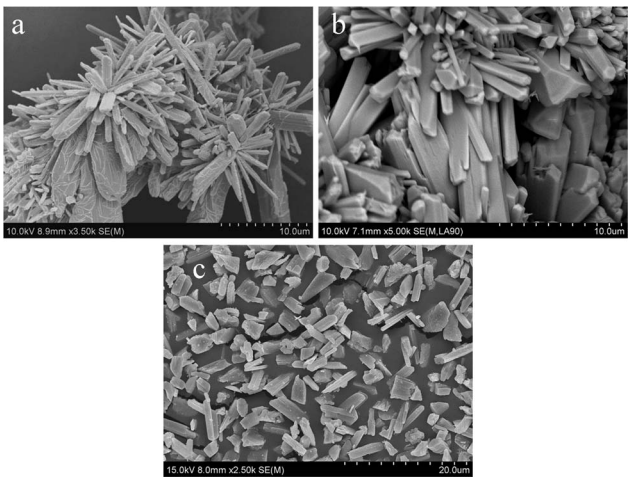

Figure 5. SEM images of samples, (a) fired for 6 h at 1300°C, (b) fired for 6 h at 1300°C with excessive $SrCl_2$ and (c) fired for 6 h at 1300°C (after acid washing).

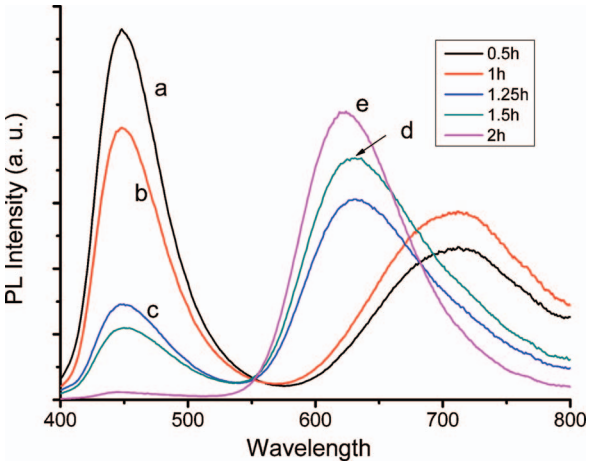

Figure 6. PL spectra of samples prepared at 1300°C for different firing durations, $\lambda_{ex.} = 290$ nm.

This reaction starts above 800°C and no significant weight loss was registered by TG analysis (see Fig. 1, curve i). In the early report of Chen[32] carried out on Li_3N+H_2 system was shown that $LiNH_2$ may form at 500°C. In this case $Li_3N/LiNH_2$ mixture will react with Si_3N_4 to form $LiSi_2N_3$.

Stage 2: Melting of $SrCl_2$ and the formation of intermediate products (900–1200°C):

In this stage molten $SrCl_2$ dissolve Eu_2O_3 to form blue-emitting $Sr_4OCl_6:Eu^{2+}$.

$$SrCl_2 + Eu_2O_3 \rightarrow Sr_4OCl_6:Eu^{2+} \quad [3]$$

Later on, $LiSi_2N_3$ reacts with $SrCl_2/Sr_4OCl_6$ to form $SrSiN_2:Eu^{2+}$,

$$LiSi_2N_3 + SrCl_2/Sr_4OCl_6:Eu^{2+} \rightarrow SrSiN_2:Eu^{2+} + LiCl(O) \quad [4]$$

According to XRD, SEM, and EDS investigation, the interaction between solid $LiSi_2N_3$ and molten $SrCl_2/Sr_4OCl_6$ ($T_{m.p.} = 1100°C$[30]) is expected to occur via the solid+liquid mechanism to form LiCl and $SrSiN_2:Eu^{2+}$ nitridosilicate phase. The blue-emitting $Sr_4OCl_6:Eu^{2+}$ yields activator ions to be homogenously distributed throughout the nitridosilicate particles. $SrSiN_2:Eu^{2+}$ formed during interaction may also incorporate Li, O and/or Cl causing its luminescence emission to be shifted.

Stage 3: The formation of $Sr_2Si_5N_8:Eu^{2+}$ phosphor (1200–1400°C)

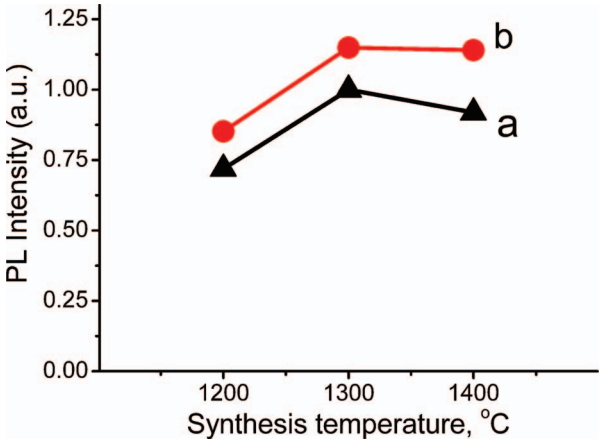

Figure 7. PL spectra of samples, (a) as-synthesized, and (b) after acid washing, $\lambda_{ex.} = 450$ nm and $\lambda_{em.} = 625$ nm.

The main route for the formation of $Sr_2Si_5N_8:Eu^{2+}$ occurs via the interaction between $SrSiN_2:Eu^{2+}$(solid) and $SrCl_2$ and may be presented as follows:

$$SrSiN_2:Eu^{2+} + SrCl_2 \rightarrow Sr_2Si_5N_8:Eu^{2+} \quad [5]$$

We do not exclude other possible chemical routes in the given system that can be valid for phosphor phase formation. More detailed mechanism can be suggested after further investigation.

Note that at elevated temperature $SrCl_2$ is being partially evaporated from the reaction sample due to its volatility. Therefore the lack of $SrCl_2$ cause incomplete interaction and results $LiSi_2N_3$ phase in the final product. Extra $SrCl_2$ compensates the possible evaporation and results single phase with improved PL performance. In our process Li_3N serves as a reduction agent for $SrCl_2$ and solid source of nitrogen which helps to carry out nitridization reaction under the atmospheric gas pressure and at relatively low temperatures. The meantime, continuous supply of nitrogen gas suppress the possible decomposition of nitride phases, and consequently prohibits evaporation of Sr and Li elements from the reaction system.

As noted above, process chemistry depends not only on the temperature but also the processing time and the presence of the liquid phases in the reaction system. Therefore at the long processing time (more than 12 hours) a partial formation of $Sr_2Si_5N_8$ phase become possible at 1100–1150°C becomes possible due to accelerated diffusion processes. This data is close to that obtained by Zeuner starting with highly active precursors.[22] On the other hand liquid phase helps to form well-crystallized $Sr_2Si_5N_8$ grains with high PL performance compared to conventional diffusion-controlled SSR or CRN methods (1500–1650°C). Moreover, the rapid growth of rod-like crystals can be also assigned to the high mobility of ions in the melt-assisted reaction environment. Another distinguishing feature of the MSSM approach is that the as-formed LiCl was being intensively evaporated during the reaction process which makes self-cleaning of the phosphor sample. According to the proposed reaction scheme, the theoretical weight loss should be ~28%, which is in full agreement with the 27–30% recorded experimentally in TG analysis.

Phosphor powder synthesized by MSSM approach shows high crystallinity and comparably better performance (high quantum efficiency and PL intensity) owing to homogenous distribution of activator ion, as well as the high phase purity of the product can be achieved.

Conclusions

We have studied the synthesis process of $Sr_2Si_5N_8:Eu^{2+}$ nitridosilicate phosphor at relatively low temperature and its photoluminescence properties using modified solid-state metathesis approach to Li_3N-$SrCl_2$- Si_3N_4-Eu_2O_3 system. In the designed system, $SrCl_2$ salt was used as an alkaline earth metal source and Li_3N as an efficient reduction agent and solid source of nitrogen. The influence of process duration and temperature was studied, and both variables were found to have significant impact on phase formation and PL properties. We have revealed that the complex nitridosilicate material is being formed via the solid+liquid interaction mechanism. The MSSM approach enabled us to reduce the temperature for synthesizing $Sr_2Si_5N_8$ nitridosilicate to 1100°C, this temperature is about 400–500°C lower than that required for the conventional synthesis routes. We first have shown that $SrCl_2$ and LiCl may be used as a flux in the synthesis process of complex alkaline-earth metal nitridosilicate phosphors. Phosphor prepared by MSSM approach at 1300°C shows excellent photoluminescence performance and thermal stability. The intensity of $Sr_2Si_5N_8:Eu^{2+}$ red-emitting phosphor synthesized by this novel method was about 115% of the commercial $YAG:Ce^{3+}$ yellow phosphor. We think that MSSM approach presented in this study has a significant promise for the scale-up development and industrial production.

Acknowledgments

This work was supported by Components & Materials Technology Development program of Ministry of Knowledge Economy (project - 10036981) and BK21 Program.

References

1. R.-J. Xie and N. Hirosaki, *Sci. Technol. Adv. Mater.*, **8**, 588 (2007).
2. K. Sakuma, K. Omichi, N. Kimura, M. Ohashi, M. D. Tanaka, N. Hirosaki, Y. Yamamoto, R.-J. Xie, and T. Suehiro, *Opt. Lett.*, **29**, 17 (2004).
3. W. Schnick, *Int. J. Inorg. Mater.*, **3**, 1267 (2001).
4. W. Schnick and H. Huppertz, *Chem. Eur. J.*, **3**, 679 (1997).
5. R.-J. Xie, N. Hirosaki, K. Sakuma, Y. Yamamoto, and M. Mitomo, *Appl. Phys. Lett.*, **84**, 5404 (2004).
6. H.-L. Li, R.-J. Xie, N. Hirosaki, T. Suehiro, and Y. Yajima, *J. Electrochem. Soc.*, **155**, J175 (2008).
7. N. Hirosaki, R.-J. Xie, K. Kimoto, T. Sekiguchi, Y. Yamamoto, T. Suehiro, and M. Mitomo, *M. Appl. Phys. Lett.*, **86**, 211905 (2005).
8. Y. Q. Li, G. deWith, and H. T. Hintzen, *J. Mater. Chem.*, **15**, 4492 (2005).
9. Y. Q. Li, A. C. A. Delsing, G. deWith, and H. T. Hintzen, *Chem. Mater.*, **17**, 3242 (2005).
10. Y. Q. Li, Ph.D. Thesis, Eindhoven University of Technology, Eindhoven, The Netherlands (2005).
11. Y. Q. Li, J. E. J. van Steen, J. W. H. van Krevel, G. Botty, A. C. A. Delsing, F. J. DiSalvo, G. deWith, and H. T. Hintzen, *Alloys Compd.*, **417**, 273 (2006).
12. X. Q. Piao, T. Horikawa, H. Hanzawa, and K.-I. Machida, *Appl. Phys. Lett.*, **88**, 161908 (2006).
13. X. Q. Piao, T. Horikawa, H. Hanzawa, and K.-I Machida, *Chem. Lett.*, **35**, 334 (2006).
14. R.-J. Xie, N. Hirosaki, T. Suehiro, F.-F. Xu, and M. Mitomo, *Chem. Mater.*, **18**, 5578 (2006).
15. X. Q. Piao, K.-I. Machida, T. Horikawa, and H. Hanzawa, *J. Electrochem. Soc.*, **155**, J17 (2008).
16. H.-L. Li, R.-J. Xie, N. Hirosaki, and Y. Yajima, *J. Electrochem. Soc.*, **155**, J378 (2008).
17. X. Piao, K.-I. Machida, T. Horikawa, and B. Yun, *J. Lumin.*, **130**, 8 (2010).
18. T. Horikawa, M. Fujitani, X. Q. Piao, H. Hanzawa, and K.-I. Machida, *J. Cer. Soc. J.*, **115**, 623 (2007).
19. T. Horikawa, X. Q. Piao, M. Fujitani, H. Hanzawa, and K.-I. Machida, *Mater. Sci. Eng.*, 012024 (2009).
20. T. Xiaoming, Z. Weidong, H. Yunsheng, and H. J. Xiaowei, *Rare Earths*, **26**, 652 (2008).
21. H. L. Li, R.-J. Xie, N. Hirosaki, T. Takeda, and G. Zhou, *Int. J. Appl. Ceram. Technol.*, **6**, 459 (2009).
22. M. Zeuner, J. Schmidt, and W. Schnick, *Chem. Mater.*, **21**, 2467 (2009).
23. M. Zeuner, F. Hintze, and W. Schnick, *Chem. Mater.*, **21**, 336 (2009).
24. K. Uheda, N. Hirosaki, Y. Yamamoto, A. Naoto, T. Nakajima, and H. Yamamoto, *Electrochem. Solid State Lett.*, **9**, H22 (2006).
25. J. Li, T. Watanabe, N. Sakamoto, H. Wada, T. Setoyama, and M. Yoshimura, *Chem. Mater.*, **20**, 2095 (2008).
26. W. Hiromu, Y. Hisanori, and K. Naoto, *J. Solid State Chem.*, **181**, 1848 (2008).
27. G. Edward and K. Richard, *Chem. Mater.*, **8**, 333 (1996).
28. W. Schipper, *Chem. Mater.*, **4**, 688 (1992).
29. C. J. Duan, X. J. Wang, W. M. Otten, A. C. A. Delsing, J. T. Zhao, and H. T. Hintzen, *Chem. Mat.*, **20**, 4, 1597 (2008).
30. H. Hagemann, F. Kubel, and H. Bill, *ChemInform Abs.*, **28**, **17**, 9236-011 (1997).
31. Y. Q. Li, N. Hirosaki, R.-J. Xie, T. Takeda, and M. Mitomo, *J. Solid State Chem.*, **182**, 301 (2009).
32. P. Chen, Z. Xiong, J. Luo, J. Lin, and K. Tan, *Nature*, **420**, 302 (2002).